

# Pulse electrodeposition of tin from sulphate bath

S. Mohan\* and N. Rajasekaran

In the present work, the pulse electrodeposition of tin from sulphate bath containing  $\text{SnSO}_4$ ,  $\text{H}_2\text{SO}_4$ , phenol sulphonic acid, gelatin and  $\beta$ -naphthol has been studied. The influences of pulsed current, duty cycle on the thickness, hardness and current efficiency of the tin deposit were studied. Electrochemical corrosion studies of the deposited tin on mild steel were conducted by potentiodynamic polarisation and electrochemical impedance spectroscopy. Cyclic voltammetry studies using potential sweep of  $10 \text{ mV s}^{-1}$  provide information about the potential ranges for tin deposition and stripping. The tin deposit on a brass substrate has been investigated using XRD, SEM and AFM. The XRD analysis revealed that the tin plated is Sn(200) and crystalline. The morphology of tin deposit is a typical fine grained and granular structure as seen from SEM and AFM.

**Keywords:** Pulse current, Tin, Hardness, Cyclic voltammetry

## Introduction

Pulse current electro deposition<sup>1</sup> has received much attention in recent years in order to improve the mechanical and electrical properties of deposits. The advantage of pulse plating are numerous, such as the reduction of porosity, lower gas content,<sup>2</sup> high purity and fine grained deposits having low electric resistance.<sup>3-4</sup> It also produces harder, pore free and nanosized deposits.<sup>5</sup> In pulse plating three parameters are independently variables, i.e. pulse current, pulse on time and pulse off time which determine the physical characteristic of the deposits obtained<sup>6</sup> from the given electrolyte.

Electrodeposition of tin from either acid sulphate or alkaline solution has been known for more than 150 years. The acid sulphate solutions are stannous sulphate, stannous fluoborate and halogen formulations. The sulphate bath contains stannous sulphate, sulphuric acid, along with agent for inhibiting the oxidation of stannous ion in the solution. Phenol sulphonic acid retard atmospheric oxidation and gelatin,  $\beta$ -naphthol produce smooth deposits.<sup>7</sup> The sulphate electrolyte is generally adopted as the first choice due to its low cost. The fluoborate bath is used when a high current density is required.<sup>8</sup>

The acidic stannous solution consumes low electricity than alkali stannous solution. In addition acidic solution can be used for electrodeposition on circuit boards with patterned photo resist. Alkali solution on the other hand can cause the photo resist to delaminate which limits their application in microelectronic packaging.<sup>9</sup>

The electrodeposition of tin in its alloyed or unalloyed form is widely used in the packaging or microelectronics

industry owing to its non-toxicity, very low melting point, excellent solderability and corrosion resistance. Since pure tin is very soft, it is widely alloyed to increase the hardness of the deposits. Alloying of tin will change the electrical properties and will hinder its use in electronic applications.<sup>10</sup>

To improve deposit morphology and adhesion during tin plating various additives are tried. These additives are basically organic compounds which include synthanol, formaldehyde, allyl alcohol,<sup>11</sup> methane sulphonic acid<sup>12-13</sup> and benzyl alcohol.<sup>14</sup> Tin and its alloy can be used as an electrode in lithium ion batteries.<sup>15-16</sup>

## Experimental

In the present study the plating electrolyte consists of stannous sulphate  $40 \text{ g L}^{-1}$ , sulphuric acid  $50 \text{ g L}^{-1}$ , phenol sulphonic acid  $40 \text{ g L}^{-1}$ ,  $\beta$ -naphthol  $2 \text{ g L}^{-1}$  and gelatin  $1 \text{ g L}^{-1}$ . To prepare the plating solution, first sulphuric acid and phenol sulphonic acid were added to the de-ionised water followed by the addition of stannous sulphate with stirring until the stannous sulphate salt was fully dissolved. Gelatin dissolved in hot water and  $\beta$ -naphthol dissolved in alcohol<sup>17</sup> were added afterwards.

The electroplating cell consisted of two electrodes, tin as the anode and brass as the cathode. The parameters used for pulse plating were given in Table 1. The pulse duty cycle and pulse peak current was calculated using the following formula<sup>18</sup>

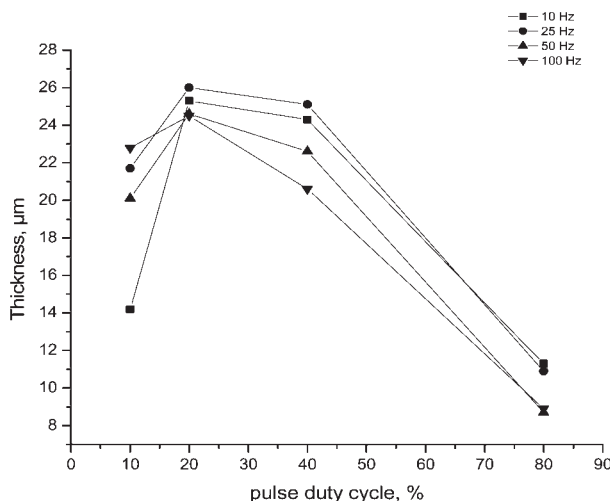
$$\text{duty cycle} = \frac{\text{on time}}{\text{on time} + \text{off time}} \times 100$$

$$\text{pulse peak current} = \frac{\text{average current}}{\text{duty cycle}} \times 100$$

The microhardness of the deposition was determined

Central Electrochemical Research Institute, Karaikudi 630 006, India

\*Corresponding author, email sanjnamohan@yahoo.com



1 Effect of pulse duty cycle at various frequencies on thickness of tin deposit

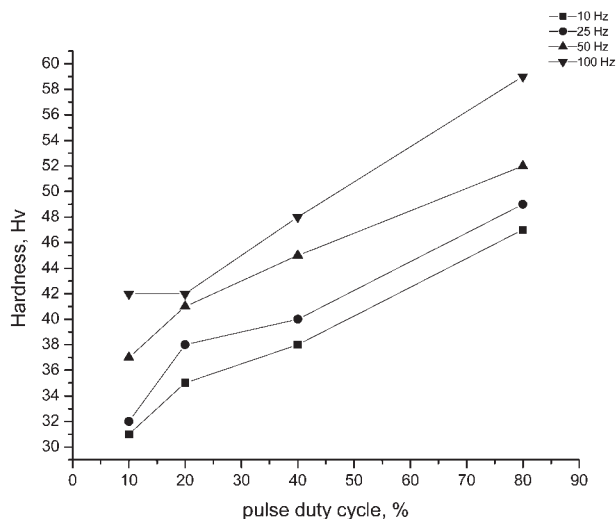
using a MH6 Everone microhardness tester. The corrosion behaviour of the deposits was studied by potentiodynamic polarisation and the electrochemical impedance spectroscopy using PARSTAT 2273 (princeton advanced electrochemical system).

Cyclic voltammetry studies of the plating solution were done using platinum wire as a working electrode, platinum foil as a counter electrode and saturated calomel electrode (SCE) as a reference electrode. The potential scan rate was set as  $10 \text{ mV s}^{-1}$ . The microstructure and surface morphology were carried out by SEM employing a Hitachi 3000 H. Structure characterisation of deposit was carried out by XRD using a Phillips diffractometer. The surface topography of Sn coatings was studied using atomic force microscopy using a molecular imaging picoscan 2100 instrument. The basic study comprised a three-dimensional representation for scanned area of  $1 \times 1 \mu\text{m}$ .

## Results and discussion

### Effect of pulse duty cycle on thickness

Figure 1 shows the effect of the pulse duty cycle on the thickness of the tin deposition obtained at various frequencies. As duty cycle increases current on time increases and off time decreases. At 10% duty cycle, peak current is flowing for less time than the 20% duty cycle. So the thickness of the coatings are high at 20% duty cycle but in 40 and 80% duty cycle the current flowing times are too high, which may not be suitable parameter for the tin deposits, so the reduced thickness is obtained. The optimum pulse duty cycle is 20%.



2 Effect of pulse duty cycle at various frequencies on hardness of tin deposit

### Effect of pulse duty cycle on hardness

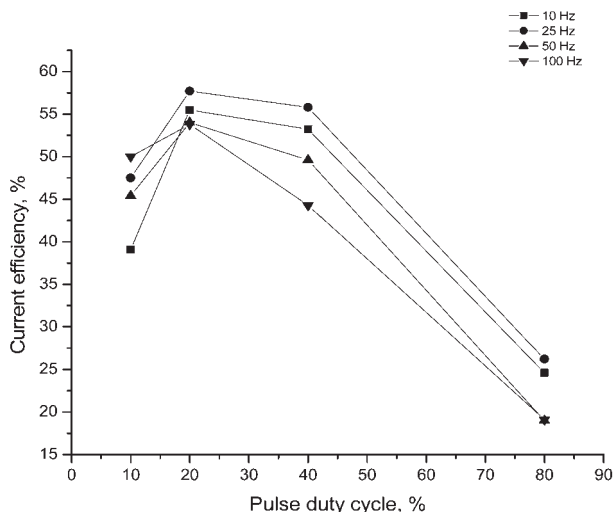
The hardness of the deposits increases when the duty cycle increased from 10 to 80%. The results are depicted in Fig. 2. As pulse frequency increases, the hardness is found to increase. During a short pulses at high frequency, a very thin pulsating diffusion layer is formed which leads to increase in nucleation rates. The reason for the thin pulsating diffusion layer is believed to be that in the immediate vicinity of the cathode the concentration pulsates with the frequency of pulse current, decreasing during the pulses and the relaxing in the interval between them. Thus, a pulsating diffusion layer exists close to the cathode. If the duration of pulse is short, the diffusion layer does not have time to extend vary far into the solution and hence surface covered with denser build up of the fine grained deposits and this leads to lower porosity and higher hardness values.<sup>19</sup> The maximum hardness values were obtained at 80% duty cycle at high frequency.

### Effect of pulse duty cycle on current efficiency

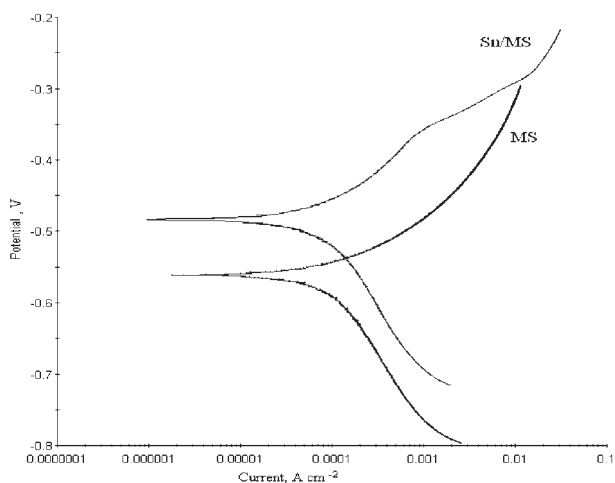
The influences of pulse duty cycle on the current efficiency of tin deposits at various frequencies are shown in Fig. 3. It has been found that the current efficiency of the tin deposits increase slightly as pulse duty cycle increase from 10 to 20% duty cycle. However an increase from 20 to 80% duty cycle decreases in the current efficiency. This may be attributed to the evolution of the hydrogen at the cathode during plating.<sup>20</sup> The maximum current efficiency has been observed at 20% duty cycle for 25 Hz frequency pulse plating at the average current  $0.15 \text{ A dm}^{-2}$

Table 1 Pulse parameters used for pulse plating on Sn

Duty cycle, %	Pulse frequency, Hz and pulse on-off times, ms				Current density, $\text{A dm}^{-2}$	
	10 Hz	25 Hz	50 Hz	100 Hz	Peak	Average
10	10–90	4–36	2–18	1–9	25.000	2.5
20	20–80	8–32	4–16	2–8	12.500	2.5
40	40–60	16–24	8–12	4–6	6.250	2.5
80	80–20	32–8	16–4	8–2	3.125	2.5



3 Effect of pulse duty cycle at various frequencies on current efficiency of tin deposit



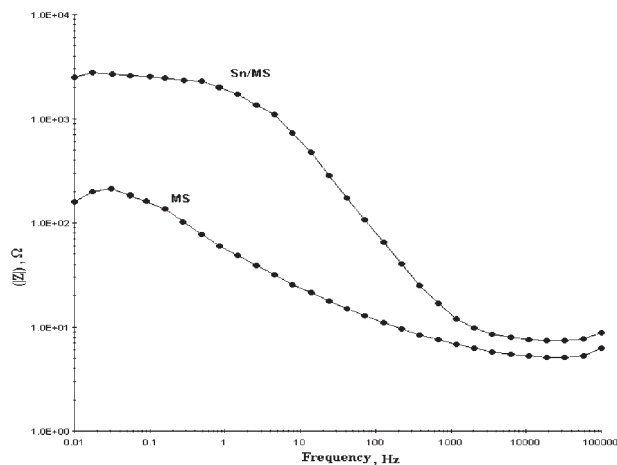
4 Potentiodynamic polarisation curves of Sn/MS and MS

Potentiodynamic polarisation studies

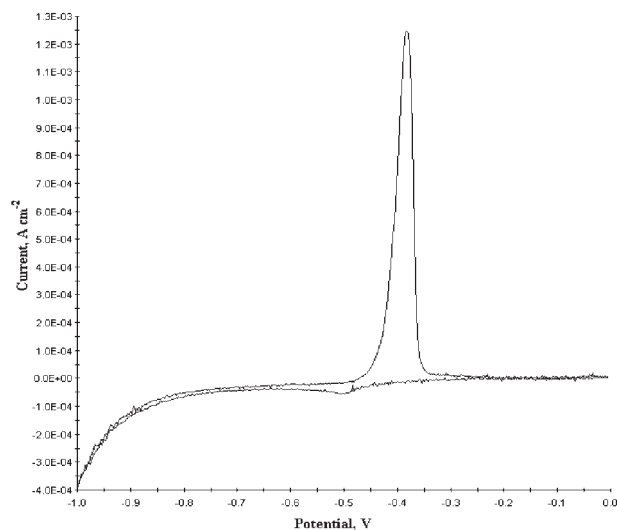
The results from the potentiodynamic polarisation of Sn coatings on the mild steel substrate in the 3.5 wt-% NaCl electrolyte are shown in Fig. 4. The curves represent the uncoated substrates and Sn coated on the mild steel substrate. The corrosion potential  $E_{corr}$  of the uncoated mild steel substrate is  $-561$  mV versus SCE and the  $E_{corr}$  shifted towards positive potential with the application of the Sn coatings and it reaches  $-483$  mV versus SCE. The corrosion current  $i_{corr}$  of the Sn coated and mild steels are  $199.3$  and  $68.36$  A. These values indicate that the Sn coating has got better corrosion resistance than the mild steel.<sup>19</sup>

Electrochemical impedance

The electrochemical impedance spectra of Sn coated system were measured with same three electrode assembly as used for the potentiodynamic polarisation experiment. The impedance was performed in a 3.5 wt-% NaCl solution at the corrosion potential. Figure 5 shows the comparative Bode impedance response of the tin coated on the mild steel and uncoated mild steel system. From these impedance spectra, it can be concluded that the absolute impedance values of the tin coated steel was higher than mild steel, which



5 Electrochemical impedance spectrums of Sn/MS and MS

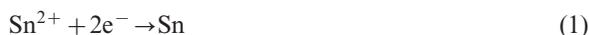


6 Cyclic Voltammetric curve of stannous sulphate bath obtained at scan rate of  $10 \text{ mV s}^{-1}$

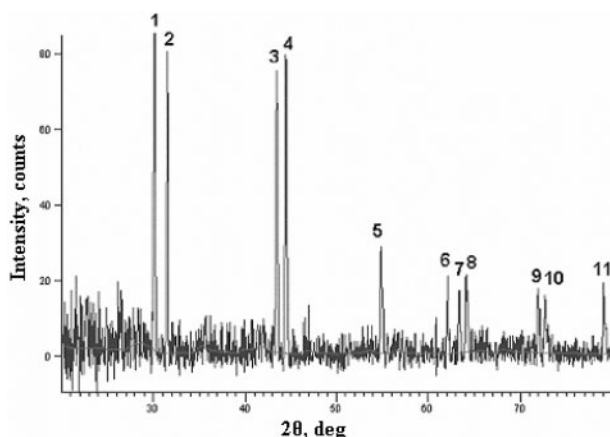
indicates that the corrosion resistance of the tin coated steel is greater than mild steel. The charge transfer resistance  $R_{ct}$  value of tin coated steel is high compared to mild steel and the double layer capacitance  $C_{dl}$  value of tin coated steel is lower than mild steel. From these results we can conclude that corrosion resistance of the mild steel improved by the coating of tin.<sup>19,21,22</sup>

Cyclic voltammetry

The cyclic voltammetry for tin electrodeposition from tin sulphate electrolyte is shown in Fig. 6. The forward scan from 0 to  $-1.0$  V versus SCE show a single reduction peak for tin deposition, correspondingly to a single, two electron transfer step



The electrodeposition of tin initiated at a potential of  $-0.492$  V versus SCE. As electrode potential become more negative, the current density reached maximum and then decreased to a plateau followed by an increasing in current density. The peak current density  $i_p$  can be associated with the complete consumption of  $\text{Sn}^{2+}$  at the electrode surface under mass transport control. Further increases in current density at more



7 X-ray diffractogram of Sn deposit

negative potential were due to the hydrogen evolution at the cathode



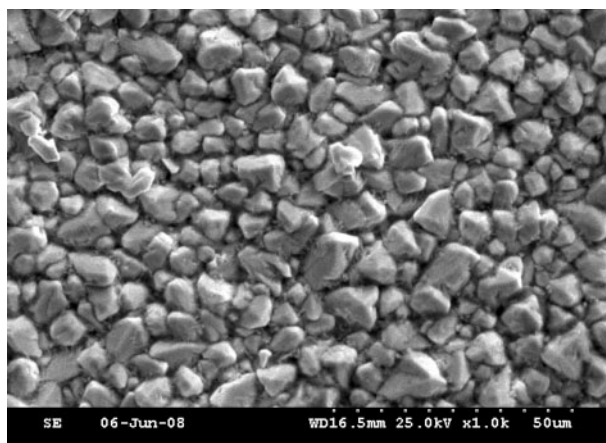
On reversing the potential sweep from  $-1.0$  to  $0$  V versus SCE, a single a stripping peak was observed. It confirms the two electron oxidation step of metallic tin to  $\text{Sn}^{2+}$  i.e. anodic stripping of tin corresponding to the reverse reaction (1). The forward and reverse curves showed no cross over i.e. no nucleation loop or over potential was required as the deposition of tin was thermodynamically favourable at a more negative potential on the brass substrate.<sup>8</sup>

### X-ray diffraction analysis

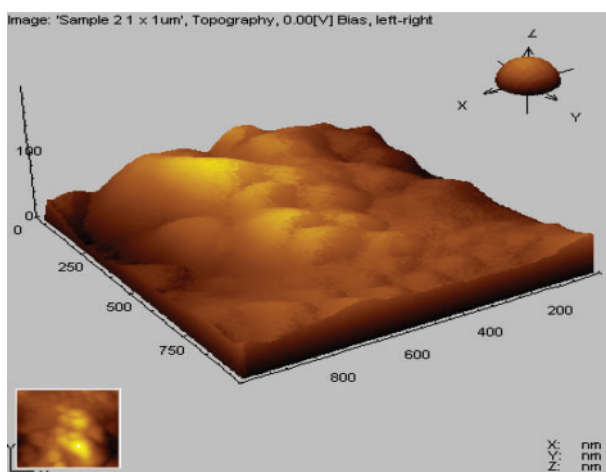
The X-ray diffractogram for the Sn plated from the sulphate bath at 20% dutycycle and 25 Hz frequency sample was shown in Fig. 7. There are 11 peaks in this spectrum. These eleven peaks can be indexed as tetragonal tin, which has lattice parameter of  $a=0.5831$  nm,  $b=0.5831$  nm and  $c=0.3181$  nm with the space group I41/amd. The XRD results are correlated with standard JCPDS data as given in Table 2. The data shows that the observed interplanar distance  $d$  values are in good agreement with the standard  $d$  values of the corresponding phases. The most intense tin peak, by far is the (200) reflection. Crystalline size  $D$  was calculated using Scherrer's formula from the full width at half maximum  $\beta$  of the peaks expressed in terms of radian.

Table 2 Data analysis from XRD pattern in Fig. 7

Peak	2-theta, °	$d$ spacing (from Fig. 7), Å	$d$ spacing (from JCPDS no. 01-086-2265), Å	Indices
1	30.1945	2.95992	2.91580	(200) <sub>Sn</sub>
2	31.5859	2.83264	2.79276	(101) <sub>Sn</sub>
3	43.4086	2.08465	2.06178	(220) <sub>Sn</sub>
4	44.4410	2.03859	2.01688	(211) <sub>Sn</sub>
5	54.9182	1.67190	1.65873	(301) <sub>Sn</sub>
6	62.0556	1.49565	1.48406	(112) <sub>Sn</sub>
7	63.3848	1.46745	1.45790	(400) <sub>Sn</sub>
8	64.1682	1.45141	1.44176	(321) <sub>Sn</sub>
9	71.9229	1.31281	1.30399	(420) <sub>Sn</sub>
10	72.7140	1.30047	1.29240	(411) <sub>Sn</sub>
11	79.0760	1.21004	1.20448	(312) <sub>Sn</sub>



8 Image (SEM) of tin deposit obtained at 20% duty cycle and 25 Hz



9 Images (AFM) (scan size  $1 \times 1 \mu\text{m}$ ) showing topography of Sn deposit on brass

$$D = 0.94\lambda / \beta \cos\theta$$

where  $\beta$  is the Full width half maximum calculated from (200) plane: average calculated crystalline size is 30.75 nm

### Surface morphology

Examination of the surface morphology by SEM (Fig. 8) showed that the Sn plated at the plating current density  $2.5 \text{ A dm}^{-2}$ , were consisted of fine grains covering the whole substrate surface. The average size of the grains was determined to be  $2\text{--}7 \mu\text{m}$  from SEM for the Sn deposits. The smaller grain sizes are facilitating the better electrochemical performance.<sup>23-24</sup> The surface topography of the Sn plated sample was carried out using atomic force microscopy (AFM). The advantage of AFM is its capacity to probe minute details related to the individual grains and inter grains region. A representative AFM picture scanned over an area of  $1 \times 1 \mu\text{m}$  of the sample prepared is shown in Fig. 9, which shows that the deposits are having finer nodular grains and uniform coverage.

### Conclusion

Pulse electrodeposition of tin on brass substrate was carried out from a tin sulphate bath at various pulse duty cycles and frequencies. The pulse plating conditions

such as duty cycle, frequency were optimised. The properties of the tin deposits such as thickness, hardness were evaluated. The current efficiency was also determined. The influence of pulse duty cycle pulse frequency on the properties of the tin deposits has been studied in detail. From the corrosion studies it is clear that tin coatings have better corrosion resistance than mild steel. From these studies, it may be concluded that the maximum current efficiency can be obtained at 20% duty cycle, when the frequency is 25 Hz.

## References

1. J. C. Puipe and F. Leeman (eds.): 'Theory and practice of pulse plating', 1st edn; 1986, Orlando FL, AESF.
2. Y. Y. Wang, C. S. Tung and C. C. Wan: *Met. Finish.*, 1980, **78**, (9), 21–25.
3. Ch. J. Raub and A. Knodler: *Plat. Surf. Finish.*, 1978, **65**, (9), 32–34.
4. N. M. Osero: *Plat. Surf. Finish.*, 1986, **73**, (3), 20–22.
5. G. Devaraj, S. Gurusiah and S. K. Seshadri: *Mater. Chem. Phys.*, 1990, **25**, 439–461.
6. S. Mohan and V. Raj: *Trans. Inst. Met. Finish.*, 2005, **83**(4), 194–198.
7. F. A. Lowenheim (ed.): 'Modern electroplating', 401–405; 1974, New York, Wiley-Interscience publication.
8. C. T. J. Low, C. Kerr, B. de Barker, J. R. Smith, S. A. Campbell and F. C. Walsh: *Trans. Inst. Met. Finish.*, 2008, **86**, (3), 148–152.
9. A. Q. He, Q. Liu and D. G. Ivey: *J. Mater. Sci: Mater Electron.*, 2008, **19**, 553–562.
10. W. E. G. Hansal, M. Halmdienst, S. Hansal, I. Boussaboua and A. Darchen: *Trans. Inst. Met. Finish.*, 2008, **86**, (2), 115–121.
11. G. I. Medvedev and N. A. Makrushin: *J. Appl. electrochem.*, 2004, **77**, 1781–1785.
12. N. M. Martyak and R. Seefeldt: *Electrochim. Acta*, 2004, **49**, 4303–4311.
13. I. S. Zavarine, O. Khaselev and Y. Zhang: *J. Electrochem. Soc.*, 2003, **150**, (4), C202–C207.
14. G. I. Medvedev, N. A. Makrushin and O. V. Ivanova: *J. Appl. electrochem.*, 2004, **77**, 1104–1107.
15. N. Tamura, R. Ohshita, M. Fujimoto, S. Fujitani, M. Kamino and I. Yonezu: *J. Power Source*, 2002, **107**, 48–55.
16. N. Tamura, M. Fujimoto, M. Kamino and S. Fujitani: *Electrochim. Acta*, 2004, **49**, 1949–1956.
17. N. V. Parthasaradhy: 'Practical electroplating hand book', 206–207; 1988, Prentice Hall, NJ, Englewood Cliffs.
18. M. S. Chandrasekar and M. Pushpavanam: *Electrochim. Acta*, 2008, **53**, 3313–3322.
19. B. Subramanian, S. Mohan and S. Jayakrishnan: *J. Appl. Electrochem.*, 2007, **37**, 219–224.
20. M. Subramanian, N. Dhanikaivelu and R. Rama Prabha: *Trans. Inst. Met. Finish.*, 2007, **85**, (5), 274–280.
21. S. Mohan and V. Raj: *Trans. Inst. Met. Finish.*, 2005, **83**, (2), 72–76.
22. V. Raj, D. Kanagaraj and S. Mohan: *Trans. Inst. Met. Finish.*, 2003, **81**, (3), 83–88.
23. W. H. Pu, X. M. He, J. G. Ran, C. R. Wan and C. Y. Jiang: *J. Electrochim. Acta*, 2005, **50**, 4140–4145.
24. D. G. Kim, H. Kim, H. J. Sohn and T. Kang: *J. Power Source*, 2002, **104**, 221–225.